

Evaluation of Time-dependent Behavior of Osaka Pleistocene Clay by Elasto-viscoplastic Finite Element Analysis

Mamoru MIMURA and Wooyoung JANG*

*Graduate Student, Faculty of Engineering, Kyoto University, Japan

Synopsis

The most difficult problem is that a delayed compression of Pleistocene clays continues even when the total overburden remains less than p_c . A new procedure is introduced to describe the delayed compression of the Pleistocene clays. A series of numerical analyses in terms of the elasto-viscoplastic finite element method is conducted to simulate those time-dependent behaviors. Furthermore, the procedure is also applied to the long-term deformation that has been monitored at the Maishima Reclaimed Island in Osaka Bay. The calculated results can also well describe the monitored long-term settlement of the each Pleistocene marine clay layers.

Keywords: Time-dependent behavior, Quasi-overconsolidated Pleistocene clay, Elasto-viscoplastic finite element analysis, settlement

1. Introduction

Osaka Bay is a heart of Kansai economy along which the urban business cities such as Osaka and Kobe are located. Urbanization has been progressed in Japan associated with the development of coastal area as well as offshore-reclaimed lands. Soft Holocene materials are normally situated near the ground surface underlain by the relatively stiff Pleistocene deposits. As most of the geotechnical problems encountered in Japan have been related to Holocene soft clay deposits, a number of knowledge on the Holocene clays and the relevant ground improvement techniques to control settlement and stability of the Holocene clay deposits are being available. On the other hand, although the occurrence of the long-term settlement of the Pleistocene deposits at the reclaimed lands along Osaka Bay has

been known, sufficient efforts to interpret the mechanism of those phenomena have not been done. It is because we had very little and limited information, and the deformation related to the compression of the Pleistocene deposits advanced slowly enough to provide countermeasure accordingly. However, large and rapid advance in settlement of the Pleistocene deposits took place at the Kansai International Airport construction site, which has made us pay a due attention to this problem. The concept of the long-term deformation was originally pointed out by Bjerrum (1967) with the idea of "delayed compression". Many attempts have subsequently been performed on the delayed, time-dependent behaviors of mainly normally consolidated clays. But the problem encountered in Osaka Bay is "long-term time-dependent settlement of the lightly overconsolidated Pleistocene clays

particularly in the region close to or less than p_c ”.

The seabed deposits of Osaka Bay have been formed due to the soil supply from the rivers on the sinking base (Kobayashi et al., 2001). Although it is common that the clay deposits formed under this environment should be normally consolidated, the Pleistocene clays in Osaka Bay exhibit slight overconsolidation with OCR of 1.2 to 1.5 in average. This seeming overconsolidation is thought not to arise from the mechanical reason but to be subjected to the effect of diagenesis, such as aging effect and/or development of cementation among clay particles. In the sense, the Pleistocene clays deposited in Osaka Bay is so-called “quasi-overconsolidated clays” without definite mechanical overconsolidation history and can also be regarded as “normally consolidated aged clays” with seeming overconsolidation.

In this paper, the characteristics of settlement in the Pleistocene deposits in Osaka Bay is discussed based on the field measurement in the reclaimed islands of Osaka Port. Particularly, the individual compression of the Pleistocene clay layers measured by the differential settlement gauges is highlighted to understand which layers strongly contribute to the long-term settlement of the Pleistocene deposits and what actually happens in the Pleistocene clay layers. The numerical assessment is discussed how the conventional procedure can evaluate the above-mentioned settlement behavior occurred in Osaka Port. Far from the textbook OC clays, they exhibit remarkable time-dependent compression even in the region less than p_c , which results in that the reclaimed lands along Osaka Bay have suffered from long-term settlement for more than 20 years (Research Committee of Seabed Deposits in Osaka Bay, 2002). A new procedure in terms of elasto-viscoplastic framework is introduced to describe those curious behaviors of the Pleistocene clays in Osaka Bay. A series of long-term consolidation tests is carried out on undisturbed clay samples. The outstanding time-dependent behaviors can again be observed even in the OC region (Mimura et al., 2001a). The authors have introduced the procedure assuming that the deformation in the OC region is no longer elastic but elasto-viscoplastic on the basis of the fact that the Osaka Pleistocene clays are normally consolidated aged ones. The compression curves derived from conventional consolidation tests are used as the reference, but the C_s in the OC region is thought to be the one caused

by the elasto-viscoplastic deformation although it is assumed to be elastic in the conventional framework. A series of finite element analyses is conducted to assess the above-mentioned long-term consolidation tests. The calculated performance can well describe the experimental time-dependent behavior in the OC region very well as well as that in the NC region. On the contrary, it is natural that the conventional elasto-viscoplastic calculation provides elastic compression in the OC region. The remarkable time-dependency of the compression curves in terms of $\varepsilon - \log p$ relations is also precisely evaluated by the proposed procedure. Finally, Maishima Reclaimed Island is selected to validate the calculated performance of the proposed method. The calculated results are compared with the in-situ measured settlement for each Pleistocene clay layers, Ma12, Ma11 and Ma10 that were measured with the differential settlement gauges in the long run.

2. In-situ Record of Long-term Settlement at Reclaimed Islands in Osaka Bay

2.1 General description of Osaka Port and subsoil condition

In Osaka Port, the harbor constructions due to reclamation were started from 1950s and the three reclaimed islands have been constructed. Fig. 1 shows the plan view of the latest Osaka Bay area together with the depths of the sea. Sakishima was constructed from 1958 to 1980, Maishima from 1973 to 1990, and Yumeshima has been constructed since 1988. There is also a plan for construction of the new reclaimed island in the offing of Yumeshima. Each island is constructed in the region where sea level is O.P. (=Osaka Pail: the standard unit of elevation in

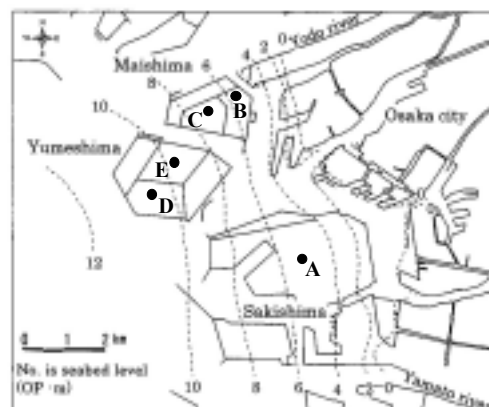


Fig. 1 Distribution of reclaimed area and reclaimed Islands

Osaka) ± 0 to -10m as shown in Fig. 1. The clayey soils dredged for the seabed and those waste disposals were used to construct these three islands. The load of reclamation is about 150 to 250kPa. The points A to E on Fig. 1 denote the monitoring locations the data from which are shown in the following section.

The representative geotechnical profiles from Ma13 to Ma10 monitored in the area are shown in Fig. 2. Ma13 is situated near the seabed and Holocene origin whereas the rest of those clays are Pleistocene origin. The liquid limit (w_L) of each marine clay deposit at the mid-depth is about 100~120%, and it is also found that every clay is highly plastic. It can be seen in the layer of Ma10 that the sea level changes cyclically during the glacial advances and retreats because the distribution of w_L shows a curved variation with higher values at the mid-depth. On the other hand, the distribution of w_L in Ma12 can be seen that the upper half of the layer has been missing. It is obvious from the fact that this upper portion of Ma12 was eroded after sedimentation. The curved variations of natural water content in Ma13 show that the consolidation has been promoted by the ground improvement in terms of vertical drains together with dewatering method. Experimental results for the consolidation yield stress, p_c , based on the standard oedometer test (STD) are also shown in Fig. 2 together with the effective overburden distribution at the time when the reclaimed fill reached up to O.P.+8m in elevation. It is clear from the Fig. 2 that the reclaimed clay layer (R) and Ma13 are under consolidation because each p_c is below the effective overburden line ($p_r = p_0 + \Delta p$). The Pleistocene clay is found to be lightly overconsolidated with the value of OCR equal to about 1.3.

2.2 Monitored settlement at Osaka Port

In this section, the record of the monitored settlement of the Pleistocene deposits at the three reclaimed islands in Osaka Port, namely, Sakishima, Maishima and Yumeshima Reclaimed Islands. The measurement points at each island are shown in Fig. 1. Fig. 3 presents the time - settlement relations for Sakishima area (Point A on Fig. 1) collected from the field measurements over 20 years since 1979. The settlement measurements in Maishima area monitored for 9 years since on the way of construction are illustrated in Fig. 4 (Point B and C

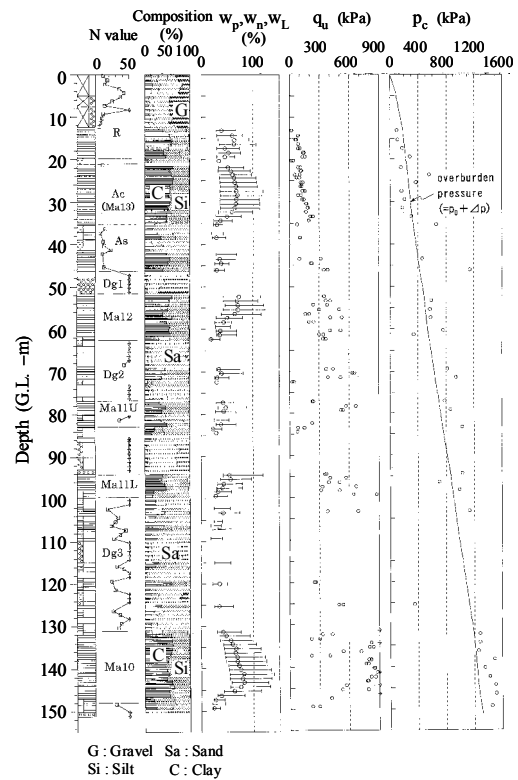


Fig. 2 Representative subsoil conditions at Osaka Port

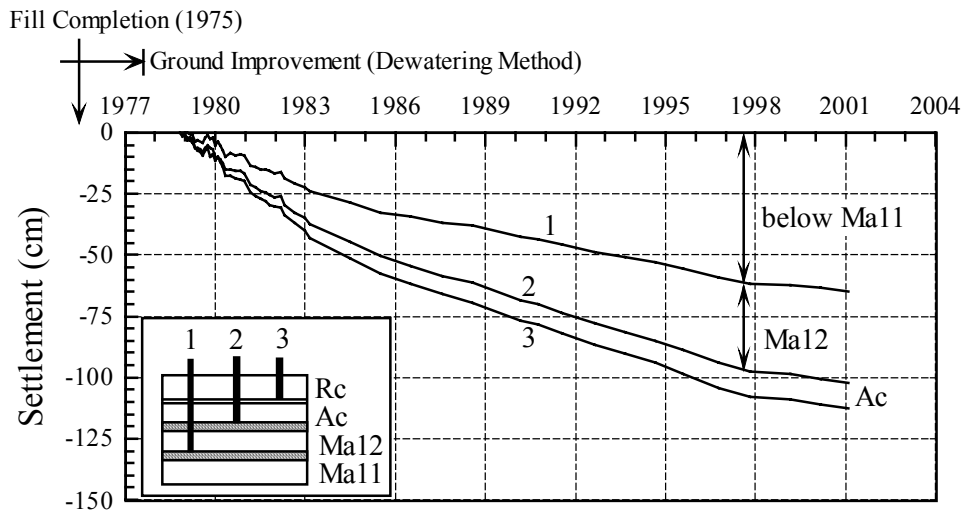
on Fig. 1). Fig. 5 shows the monitored settlement in Yumeshima Reclaimed island for about 10 to 14 years (Point D and E on Fig. 1). Measurement at Sakishima is conducted with the double tube settlement gauges (Fig. 3(a)) and with the leveling of the superstructures supported by the piles into different gravel strata (Fig. 3(b)). It was conducted with the differential settlement gauges at Maishima Reclaimed Island for both Point B and C. Measurement at Yumeshima is conducted with the double tube settlement gauges and with the leveling of the top of the rod penetrating in to the top of the Pleistocene deposit for both Point D and E.

The subsoil conditions of three sites are almost similar shown in Fig. 2. The construction sequence and the way of reclamation are also the same for all sites, namely, the dredged clayey soils, the good quality sandy soils and construction disposals were used for reclamation and filling respectively. The vertical drains with dewatering method were used to promote consolidation for Ma 13 and the dredged clay layer. Furthermore, the loading stresses to the Pleistocene deposits at both sites are also the same with the maximum value of $\Delta p = 250$ kPa. The elevation of the seabed at Sakishima is about O.P.-6m

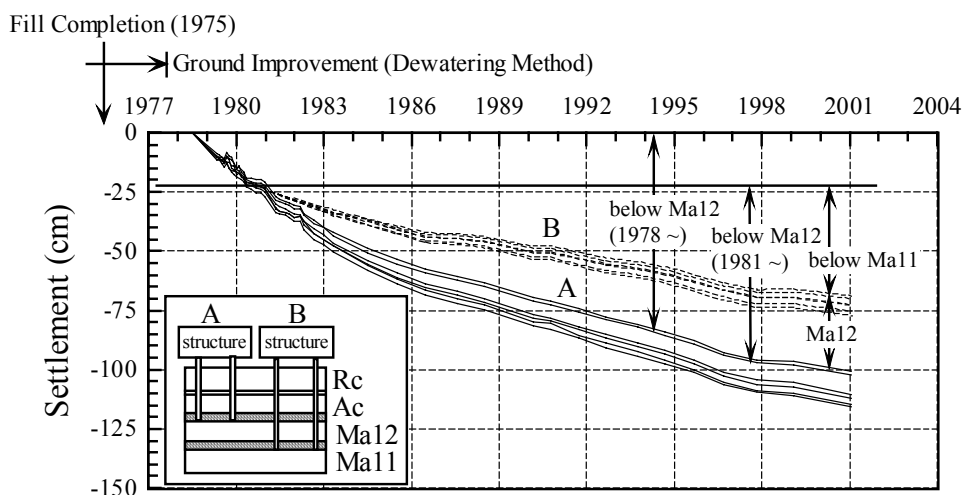
and the height of the ground surface is about O.P.+14m in elevation. At Maishima Reclaimed Island, the elevation of the seabed is also about O.P. -6 to -7m and the filling with dredged materials and construction disposals was carried out to the height of O.P.+8 to +10m.

The settlement of the deposits below Ac (Ma13), Ma12, and Ma11 at Sakishima was measured and the compressions of Ac, Ma12 and Ma11 deposits were calculated based on these measured data as shown in Fig. 3. As the measurement was started about 4 years after the completion of filling, the large compression of the Holocene clay layer is thought to be completed during this period. Then, the subsequent compression

of the Holocene clay layer is not so significant with a slight advance due to secondary consolidation. On the other hand, the settlement for all Pleistocene deposits is progressed with about 5cm/year and the total settlement amounts to about 1m for 20 years from the start of measurement. It is true a large compression occurs in Ma12 but it should be emphasized that the settlement of Ma11 and its underlying deposits taking place since the end of reclamation is found to be 2/3 of that of the total settlement of the Pleistocene deposits. The same results are obtained for the other site in Sakishima based on the leveling measurement of the superstructures supported by the piles in to the different gravel strata as shown in Fig. 3(b).

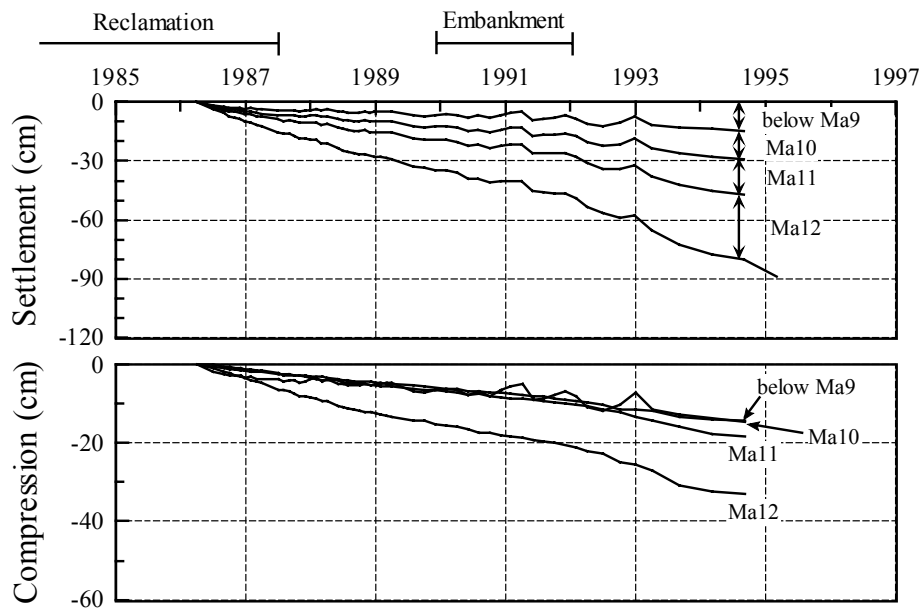


(a) Double tube settlement gauges

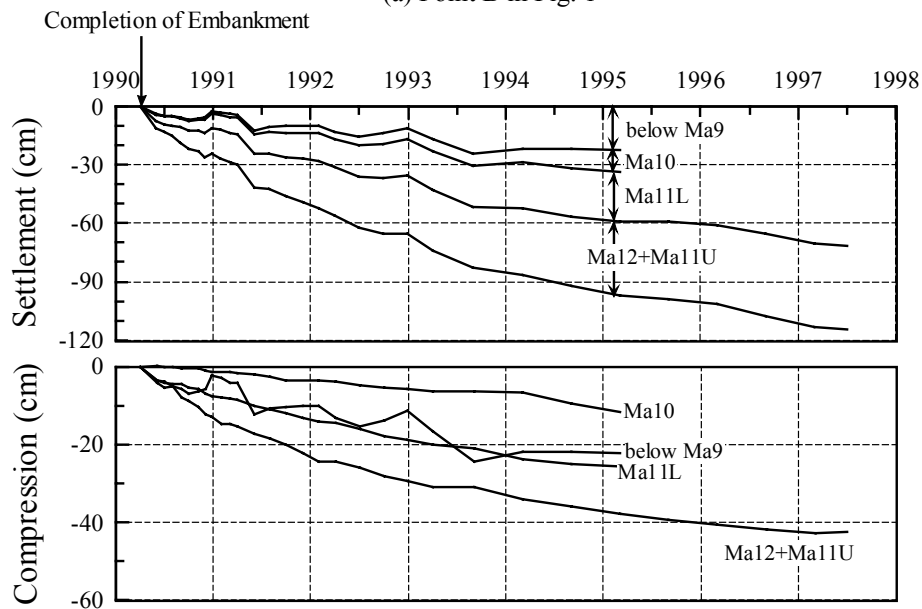


(b) Leveling of the superstructure supported by piles

Fig. 3 Measured time-settlement relations at Sakishima Reclaimed Island (point A in Fig. 1)



(a) Point B in Fig. 1

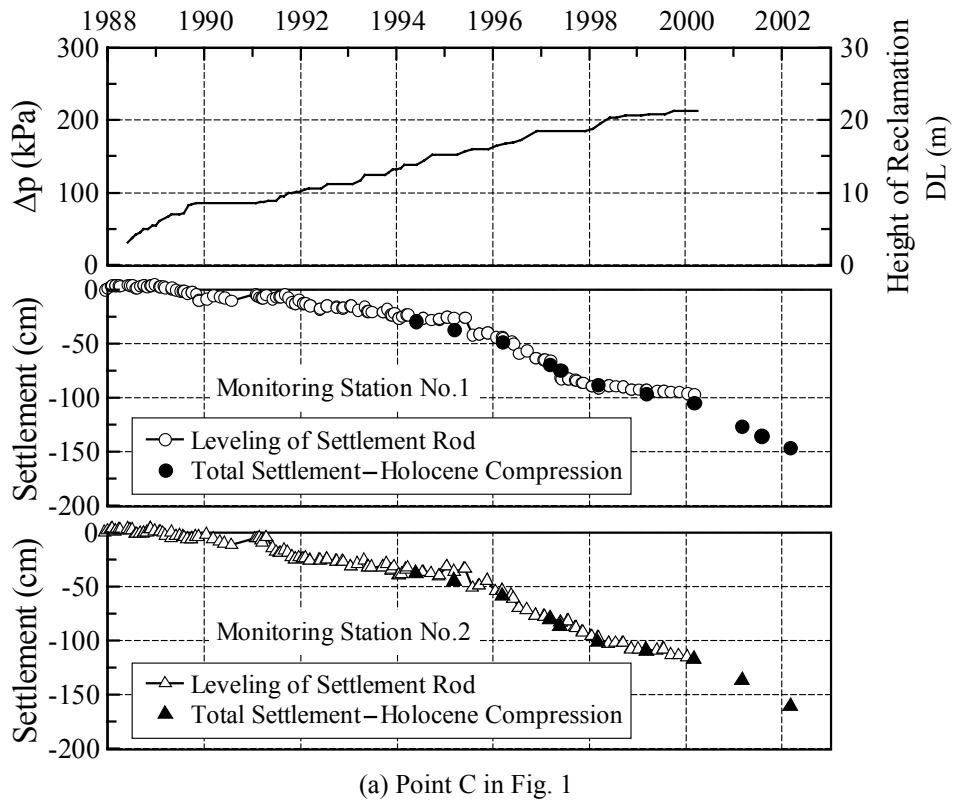


(b) Point C in Fig. 1

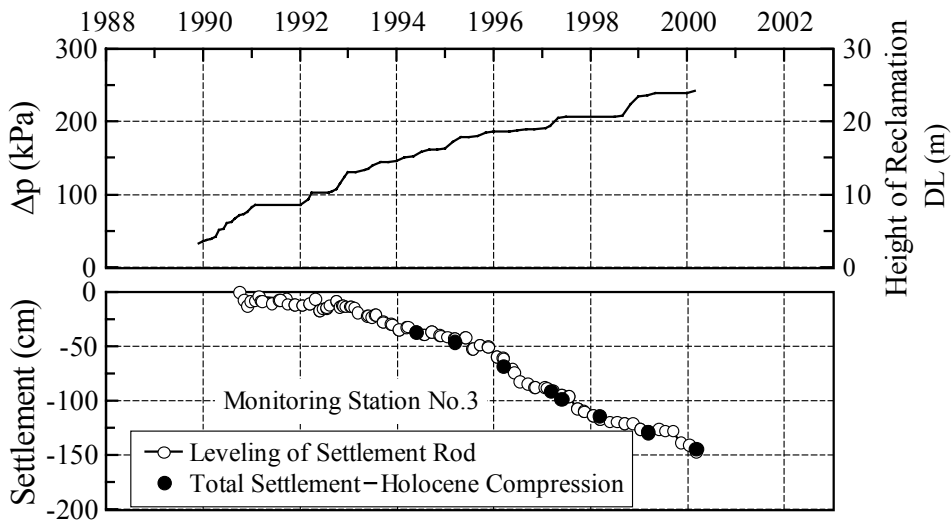
Fig. 4 Measured time-settlement relations at Maishima Reclaimed Island with differential settlement gauges

Fig. 4 shows the settlement of the deposits below Ma12, Ma11, Ma10 and Ma9 at Maishima Reclaimed Island and the compressions of Ma12, Ma11, Ma10 and Ma9 layers are calculated based on these measured data. Fig. 4(a) shows the measured advance in settlement since the end of reclamation. Those data denote the overall compression of each layer from the

virgin state. It is a pity that the records were quitted due to damage of the gauges, but it can be seen that large settlements had continued in the Pleistocene layers at Maishima Reclaimed Island. Particularly, a due attention should be paid to the fact that the compression occurred even in Ma9 and its underlying deposits the stress conditions of which remain less



(a) Point C in Fig. 1



(b) Point D in Fig. 1

Fig. 5 Measured time-settlement relations at Yumeshima Reclaimed Island with differential settlement gauges

than p_c . The settlement for all the Pleistocene deposits is progressed in about 15cm/year and the total settlement amounts to about 120cm for 7 years from start of the measurement. Fig. 4(b) shows the measured time - settlement relations at the other point in Maishima Reclaimed Island. As same as the data shown in Fig. 4(a), steady and continuous

compression can be seen for each Pleistocene clay layers. Again, we have a certain amount of settlement even for Ma9 and its underlying deposits here. The settlement of Ma11 and its underlying deposits is also found to be 2/3 of that of the total settlement of the Pleistocene deposits. The rate of settlement here is about 10cm/year and the total settlement amounts to

about 90cm for 9 years from start of the measurement.

Time - settlement relations monitored in Yumeshima Reclaimed Island are shown in Fig. 5. Here dredged slurry was used as reclaimed materials. As the level of the muddy water has been kept higher inside the reclaimed island than that of the water level of the sand mat, the difference of those water levels cause the increase in overburden pressure for the original foundation. The intensity of the overburden increment due to reclamation is calculated based on the measured density and elevation of the dredged slurry together with the above-mentioned effect of the difference in water levels. As only the total settlement of the Pleistocene deposit was monitored in Yumeshima Reclaimed Island, the contribution of the individual layers cannot be discussed. Almost no settlement occurred in the early stage of construction with the load intensity of about 100kPa, but when the overburden pressure became larger than 100kPa the compression of the Pleistocene deposits began and it was accelerated once the overburden pressure exceeded 150kPa. The total settlement of the Pleistocene deposits is 1.5m for 14 years at Point D and 10 years at Point E. Mimura et al. (2001b) showed that 5cm of settlement advanced for 1 year (1994 to 1995) with a constant overburden pressure of 105 to 118kPa that is less than p_c . It means that the time dependent behavior occurs in the Pleistocene clay deposits even when the total stress does not exceed the consolidation yield stress, p_c .

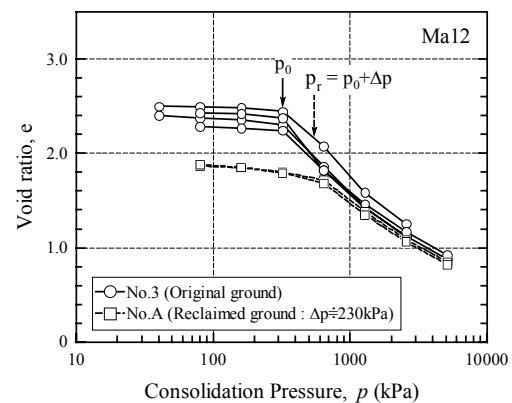
The same phenomena for settlement are observed at some other measuring points in the reclaimed islands in Osaka Port (Research Committee of Seabed Deposits in Osaka Bay, 2002) and the characteristics of the settlement behavior can be summarized as follows:

- (1) Long-term settlement has continued for about 7 to 20 years after the end of construction.
- (2) The settlement occurred even in the lower overconsolidated Pleistocene clay deposits.
- (3) Although the stresses in the lower Pleistocene layers remain below p_c , the long-term settlement occurred in the overconsolidated region.

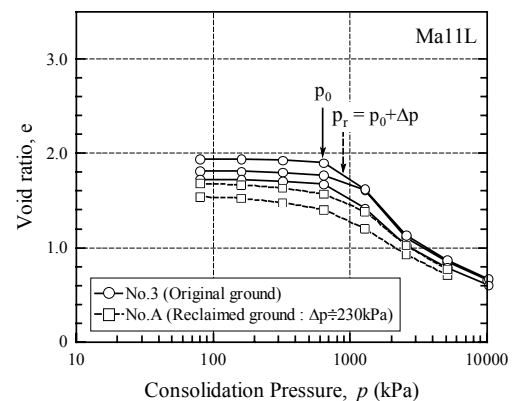
2.3 Transformation of $e - \log p$ curves due to reclamation

Fig. 6 shows that the comparison of $e - \log p$ derived from the experiments on the samples

obtained from the virgin and the reclaimed deposits at Maishima Reclaimed Island. The result of $e - \log p$ for the virgin clay is derived from the boring data at the side of Maishima Reclaimed island in 1993. On the other hand, the result of $e - \log p$ for the sample obtained from the Maishima Reclaimed Island is derived from the inside of the island after 10 years since the end of construction. It is inferred that the load of reclamation is about 230kPa. Let us compare the results of $e - \log p$ for Ma12 with that for Ma11. The data of standard consolidation tests in the high



(a) Ma12



(b) Ma11

Fig. 6 Transformation of $e - \log p$ curves due to reclamation

plasticity portion, $w_L \geq 100\%$ are used for comparison. In Fig. 6, the plots with the open circle denote the performance of the virgin clay, and those compressed clay obtained from the inside of the reclaimed land respectively. Here, the points of initial overburden, p_0 , and the present overburden, p_r ($= p_0 + \Delta p$) in the reclaimed land are also shown in Fig. 6. As is clearly seen in the Fig. 6, p_r is placed in the normally consolidated region ($p_r \geq p_c$) for Ma12 while it is placed in the transient region ($p_r \cong p_c$) for

Ma11L. The samples obtained from Maishima site has been consolidated with the overburden stress of p_r that is larger than p_c for Ma12.

The performance of $e - \log p$ for the samples obtained from the reclaimed area coincides with that for the virgin clay at p_r without significant loss of void ratio in the recompression process and rejoins the normally consolidated line. It can be recognized that the consolidation behavior of Ma12 follows the conventional consolidation theory for overconsolidated and normally consolidated clays in this particular case. On the contrary, the present overburden, p_r remains in the transient range, ($p_r \cong p_c$) for Ma11. The performance of $e - \log p$ for the samples obtained from the reclaimed area differs from that for the virgin clay at p_r . Void ratio, e for the clay from the reclaimed area is smaller than that for the virgin clay at p_r . It is thought when the clay is consolidated with the overburden close to p_c , the non-negligible compression takes place and the values of e at p_r for the virgin clay does not coincide with that for the overconsolidated clay whose void ratio is much smaller. This phenomenon suggests that the Pleistocene clay consolidated with the overburden near p_c possibly undergoes more compression than that is expected as an elastic deformation. It is also very interesting to note the above-mentioned fact that the overconsolidated Pleistocene clay situated deep in the marine foundation exhibits significant settlement even if they remain in the overconsolidated region supports the experimental findings shown in Fig. 6.

3. Elasto-viscoplastic Finite Element Analysis

3.1 Constitutive model and formulation

The elasto-viscoplastic constitutive model used in this paper was proposed by Sekiguchi (1977). Sekiguchi et al. (1982) modified the model to a plane-strain version. The viscoplastic flow rule for the model is generally expressed as follows:

$$\dot{\varepsilon}_{ij}^p = \Lambda \frac{\partial F}{\partial \sigma_{ij}} \quad (1)$$

in which F is the viscoplastic potential and Λ is the proportional constant. Viscoplastic potential F is defined as follows:

$$F = \alpha \cdot \ln \left[1 + \frac{\dot{v}_0 \cdot t}{\alpha} \exp \left(\frac{f}{\alpha} \right) \right] = v^p \quad (2)$$

in which α is a secondary compression index, \dot{v}_0 is the reference volumetric strain rate, f is the function in terms of the effective stress and v^p is the viscoplastic volumetric strain. The concrete form of the model is shown in the reference (Mimura and Sekiguchi, 1986). The resulting constitutive relations are implemented into the finite element analysis procedure through the following incremental form:

$$\{\Delta \sigma'\} = [C^{ep}] \{\Delta \varepsilon\} - \{\Delta \sigma^R\} \quad (3)$$

Where $\{\Delta \sigma'\}$ and $\{\Delta \varepsilon\}$ are the associated sets of the effective stress increments and the strain increments respectively, and $[C^{ep}]$ stands for the elasto-viscoplastic coefficient matrix. The term $\{\sigma^R\}$ represents a set of 'relaxation stress', which increases with time when the strain is held constant. The pore water flow is assumed to obey isotropic Darcy's law. In relation to this, it is further assumed that the coefficient of permeability, k , depends on the void ratio, e , in the following form:

$$k = k_0 \cdot \exp \left(\frac{e - e_0}{\lambda_k} \right) \quad (4)$$

in which k_0 is the initial value of k at $e=e_0$ and λ_k is a material constant governing the rate of change in permeability subjected to a change in the void ratio. Note that each quadrilateral element consists of four constant strain triangles and the nodal displacement increments and the element pore water pressure is taken as the primary unknowns of the problem. The finite element equations governing those unknowns are established on the basis of Biot's formulation (Christian, 1968, Akai and Tamura, 1976), and are solved numerically by using the semi-band method of Gaussian elimination.

3.2 Compression modeling for Pleistocene clays

In the present study, a new assumption for compression is introduced to the conventional procedure. Based on the in-situ measured data, the long-term settlement has been found to take place in the reclaimed islands of Osaka Port even in the Pleistocene clay layers that do not undergo the plastic

yielding (Mimura et al., 2001b). As is also stated, the seabed deposits of Osaka Bay have been formed due to the soil supply from the rivers on the sinking base. Therefore, those sediments such as the Pleistocene clays should be normally consolidated although they exhibit the apparent overconsolidation with OCR of 1.2 to 1.5. The authors consider those Pleistocene clays as “normally consolidated aged clays” with seeming overconsolidation due to diagenesis effect. In the sense, the following assumption is introduced: The Pleistocene clays in Osaka Bay is “normally consolidated aged clays” that exhibit the elasto-viscoplastic behavior even in the region $p_0 + \Delta p \leq p_c$ as schematically shown in Fig. 7, while an elastic behavior is assumed to occur in this region by the conventional constitutive models. Here, the Pleistocene clays are assumed to exhibit a time-dependent behavior not only in the normally consolidated but also in the overconsolidated region. But once those clays undergo additional loading, the corresponding stress should be p_c and unloading - reloading region clays exhibit elastic behavior as is conventionally assumed. In short, only the virgin loading for the Pleistocene clays can provide elasto-viscoplastic behavior and once clays experience additional load increment Δp , they exhibit the conventional OC behavior in the range of p_0 to $p_0 + \Delta p$.

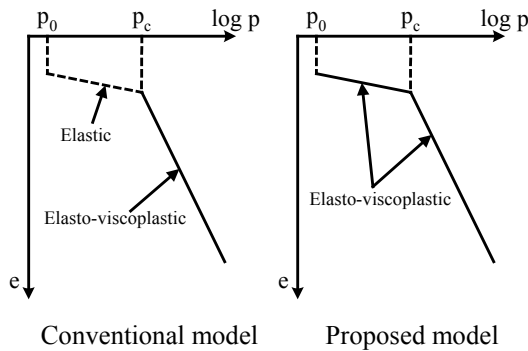


Fig. 7 Assumption for the elasto-viscoplastic behavior for the Pleistocene clays

3.3 Simulation of long-term consolidation tests on quasi-overconsolidated Pleistocene clays

In order to confirm the validity of the framework, a series of laboratory long-term consolidation tests on undisturbed aged clay samples are numerically simulated by the elasto-viscoplastic finite element method with the proposed procedure. The secondary compression index, α governing the time-dependant

behavior is determined using the relationship of the compression index, C_c in the NC region (Ishii et al., 1984). Mesri and Godlewski (1977) explained that the value of α was small at effective stresses less than consolidation yield stress, increased as the consolidation yield stress was approached. Tanaka (2003) also pointed out the same characteristics between α and the relative yield stress index, defined by $(p-p_0)/(p_c-p_0)$ in the quasi-overconsolidated region ($p_0 < p < p_c$). In the present analysis, it is assumed that α is 0.1 times where the consolidation pressure is equal to p_0 than the prescribed value in the NC region, and increase with the increase in the relative yield stress index, while α remains constant irrespective of the stress level in the NC region. Fig. 8 shows the adopted relationship between α and the relative yield stress index schematically. The rate of consolidation is another important factor to control the process of deformation. The characteristic time, t_c in the constitutive model is closely related to the coefficient of consolidation, c_v . The value of t_c is determined both for quasi-overconsolidated region ($p_0 < p < p_c$) and the NC region ($p > p_c$) as a dissipation time of excess pore water pressure, which is calculated using c_v in the NC region obtained from conventional consolidation test. It is because of the fact that c_v in quasi-overconsolidated region ($p_0 < p < p_c$) is approaching that of the NC region, while c_v in the OC ($p < p_0$) region is sufficiently large compared to that in the NC region. In short, the same value for t_c is introduced for both in quasi-overconsolidated ($p_0 < p < p_c$) and NC region ($p > p_c$) in the present study. Based on the parameters, α and t_c , the reference volumetric strain rate, \dot{v}_0 becomes a constant maximum value in the NC region ($p > p_c$). In the quasi-overconsolidated region ($p_0 < p < p_c$), \dot{v}_0 decrease with the decrease in the relative yield stress index, and at $p=p_0$ the value becomes as 0.1 times as that of the NC region.

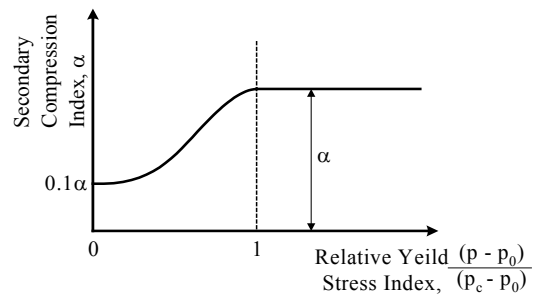
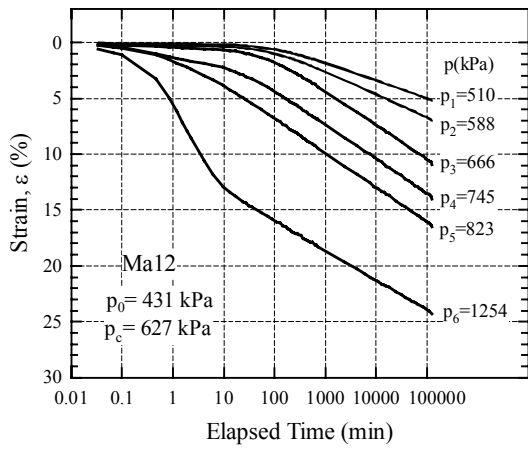
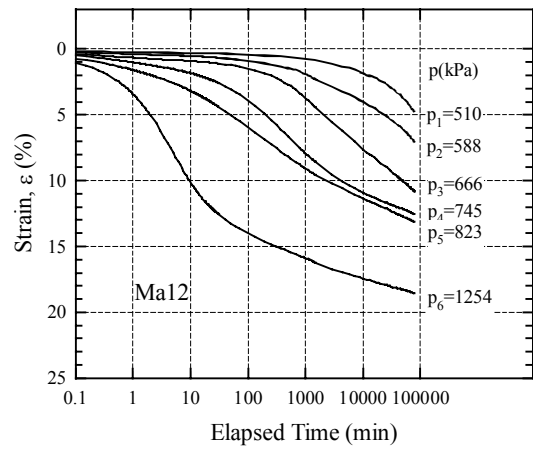


Fig. 8 Assumed relationship between the coefficient of secondary compression index and the relative yield stress

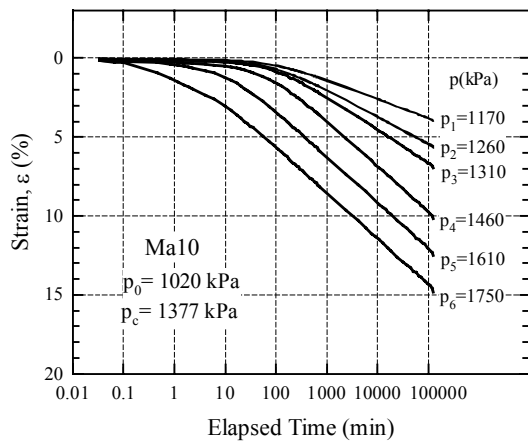


(a) Calculated results

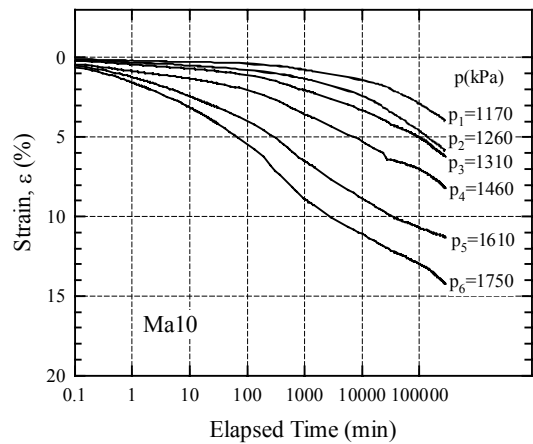


(b) Experimental results

Fig. 9 Relationships between strain and time for Ma12

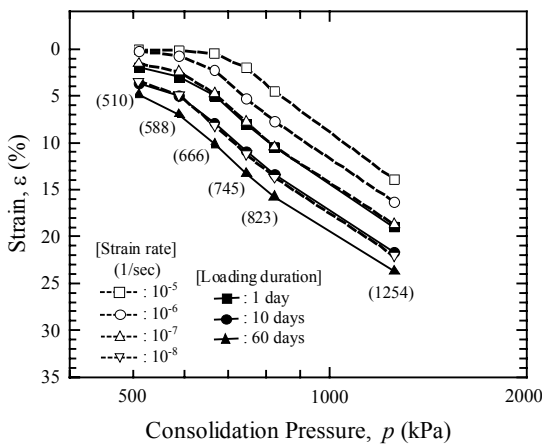


(a) Calculated results

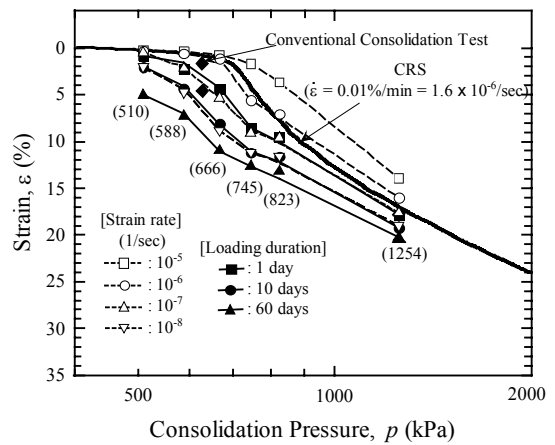


(b) Experimental results

Fig. 10 Relationships between strain and time for Ma10



(a) Calculated results



(b) Experimental results

Fig. 11 ϵ - $\log p$ curves of equi-strain rate for Ma12

The calculated performance of compression strains with time at various stress level for Ma12 and Ma10 is shown in Fig. 9(a) and 10(a). For the cases that the stress states become normally consolidated

due to load increment, the secondary compressions occur gradually after a significant increase at the early stage of consolidation. On the contrary, it can be seen that the compressions are developed with

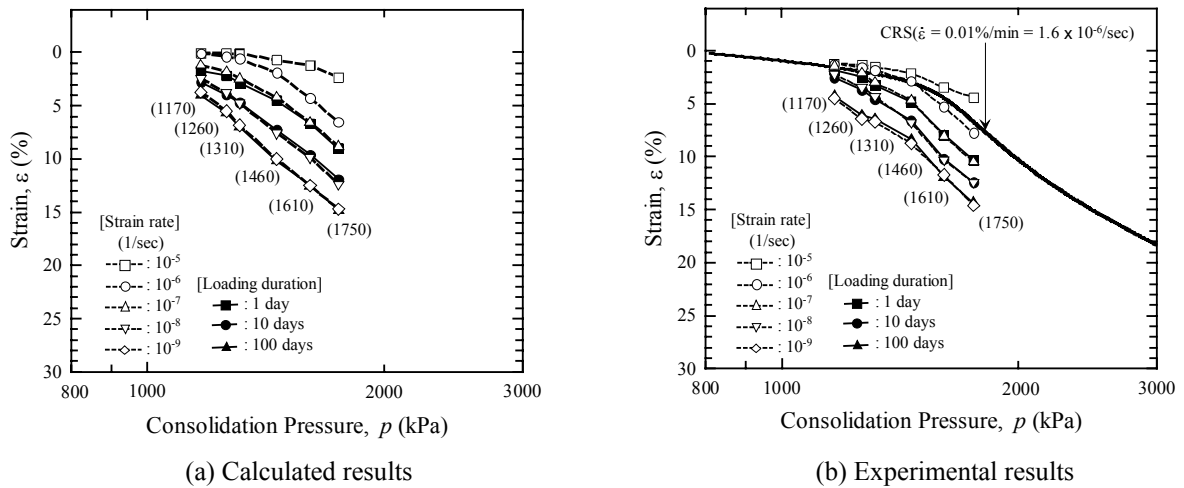


Fig. 12 ε - $\log p$ curves of equi-strain rate for Ma10

time for the cases that the total overburden stresses remain within the quasi-overconsolidated region. The calculated results coincide well with the laboratory long-term consolidation test results (Fig. 9(b) and 10(b)).

Fig. 11 and 12 show the comparison of the experimental results and the calculated results in terms of ε - $\log p$ relations for Ma12 and Ma10, respectively. It can be seen that the delayed compression takes place for all results with the elapse of time, as well as the ε - $\log p$ curves are placed lower with decreasing the strain rate. It is also quite interesting that the sharp bending point denoted by consolidation yield stress becomes more dull and lower with the decrease in strain rate. In particular, it is noteworthy that the delayed compression is shown

not only the NC region but also the quasi-overconsolidated region for all cases. As is seen Fig. 11 and 12, the present procedure can well describe the experimental time-dependant behavior of the Pleistocene clays in Osaka Bay.

4. Numerical Assessment of Long-term Settlement of the Reclaimed Marine Foundation at Maishima in Osaka Bay

4.1 Monitored long-term settlement of Maishima Reclaimed Island

In Osaka Port, Maishima Reclaimed Island has started to be constructed in 1969's by dumping the dredged disposals and at after 7 years, sand drains were driven following the set of sand mat. Then the

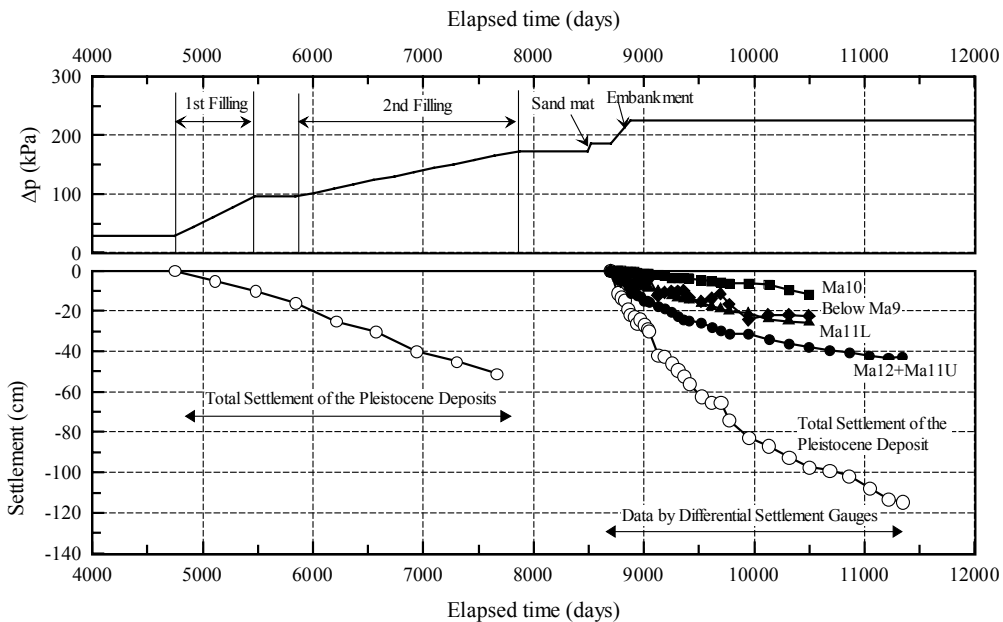


Fig. 13 Construction sequence and the monitored settlement at Maishima Reclaimed Island

Table 1 Input parameters for the finite element analysis

MTYP	Quasi-OC region				NC region				M	v'	σ_{vo}' (kPa)	σ_{vc}' (kPa)	e _o	k _o (m/day)	λ_k	
	λ_{OC}	κ_{OC}	α_{OC}	\dot{v}_{oOC} (day ⁻¹)	λ_{NC}	κ_{NC}	α_{NC}	\dot{v}_{oNC} (day ⁻¹)								
23	0.077	0.008	1.15×10^{-3}	2.49×10^{-7}	0.768	0.077	1.15×10^{-2}	2.49×10^{-6}	1.3	0.36	285	385	2.34	8.64×10^{-5}	0.768	Ma12
22	0.109	0.011	1.64×10^{-3}	3.55×10^{-7}	1.089	0.109	1.64×10^{-2}	3.55×10^{-6}	1.3	0.36	305	412	2.32	8.64×10^{-5}	1.089	Ma12
21	0.084	0.008	1.60×10^{-3}	3.46×10^{-7}	0.842	0.084	1.60×10^{-2}	3.46×10^{-6}	1.3	0.36	325	439	1.63	8.64×10^{-5}	0.842	Ma12
20	0.02	0.002	4.81×10^{-4}	1.04×10^{-7}	0.204	0.020	4.81×10^{-3}	1.04×10^{-6}	1.3	0.36	346	467	1.12	8.64×10^{-5}	0.204	Ma12
19	—	—	—	—	—	—	—	—	—	0.33	429	558	0.93	2.16×10^{-2}	—	Sand
18	0.031	0.003	6.82×10^{-4}	1.03×10^{-6}	0.308	0.031	6.82×10^{-3}	1.03×10^{-5}	1.3	0.36	513	667	1.26	6.05×10^{-5}	0.308	Ma11U
17	0.024	0.002	5.96×10^{-4}	8.97×10^{-7}	0.243	0.024	5.96×10^{-3}	8.97×10^{-6}	1.3	0.36	537	698	1.04	6.05×10^{-5}	0.243	Ma11U
16	—	—	—	—	—	—	—	—	—	0.33	582	728	0.93	2.16×10^{-2}	—	Sand
15	0.077	0.008	1.40×10^{-3}	1.34×10^{-6}	0.774	0.077	1.40×10^{-2}	1.34×10^{-5}	1.3	0.36	625	750	1.76	5.18×10^{-5}	0.774	Ma11L
14	0.049	0.005	9.77×10^{-4}	9.36×10^{-7}	0.490	0.049	9.77×10^{-3}	9.36×10^{-6}	1.3	0.36	649	779	1.51	5.18×10^{-5}	0.490	Ma11L
13	0.024	0.002	6.36×10^{-4}	6.09×10^{-7}	0.243	0.024	6.36×10^{-3}	6.09×10^{-6}	1.3	0.36	676	811	0.91	5.18×10^{-5}	0.243	Ma11L
12	—	—	—	—	—	—	—	—	—	0.33	865	1038	0.93	2.16×10^{-2}	—	Sand
11	0.063	0.006	1.33×10^{-3}	2.15×10^{-7}	0.629	0.063	1.33×10^{-2}	2.15×10^{-6}	1.3	0.36	1051	1261	1.45	2.59×10^{-5}	0.629	Ma10
10	0.081	0.008	1.47×10^{-3}	2.37×10^{-7}	0.812	0.081	1.47×10^{-2}	2.37×10^{-6}	1.3	0.36	1075	1290	1.87	2.59×10^{-5}	0.812	Ma10
9	0.092	0.009	1.43×10^{-3}	2.30×10^{-7}	0.916	0.092	1.43×10^{-2}	2.30×10^{-6}	1.3	0.36	1102	1322	2.21	2.59×10^{-5}	0.916	Ma10
8	0.056	0.006	1.25×10^{-3}	2.01×10^{-7}	0.560	0.056	1.25×10^{-2}	2.01×10^{-6}	1.3	0.36	1126	1351	1.24	2.59×10^{-5}	0.560	Ma10
7	—	—	—	—	—	—	—	—	—	0.33	1226	1471	0.93	2.16×10^{-2}	—	Sand
6	0.044	0.004	1.12×10^{-3}	6.01×10^{-8}	0.438	0.044	1.12×10^{-2}	6.01×10^{-7}	1.3	0.36	1330	1596	0.95	3.46×10^{-5}	0.438	Ma9
5	0.072	0.007	1.51×10^{-3}	8.08×10^{-8}	0.716	0.072	1.51×10^{-2}	8.08×10^{-7}	1.3	0.36	1352	1622	1.37	3.46×10^{-5}	0.716	Ma9
4	0.072	0.007	1.51×10^{-3}	8.08×10^{-8}	0.716	0.072	1.51×10^{-2}	8.08×10^{-7}	1.3	0.36	1389	1667	1.37	3.46×10^{-5}	0.716	Ma9
3	0.064	0.006	1.22×10^{-3}	6.54×10^{-8}	0.638	0.064	1.22×10^{-2}	6.54×10^{-7}	1.3	0.36	1420	1704	1.61	3.46×10^{-5}	0.638	Ma9
2	0.064	0.006	1.22×10^{-3}	6.54×10^{-8}	0.638	0.064	1.22×10^{-2}	6.54×10^{-7}	1.3	0.36	1446	1735	1.61	3.46×10^{-5}	0.638	Ma9
1	0.095	0.010	2.21×10^{-3}	1.18×10^{-8}	0.950	0.095	2.21×10^{-2}	1.18×10^{-7}	1.3	0.36	1464	1757	1.15	3.46×10^{-5}	0.950	Ma9

large-scale filling was started with dredged materials. Vertical drains were also driven in the dredged materials to promote dewatering from the dredged materials followed by the final embankment construction. The construction sequence is shown in Fig. 13 together with the monitored data. During the 1st and 2nd filling with dredged materials, the total settlement of the Pleistocene deposits was monitored by double tube settlement gauges. Again during the final sand mat setting prior to embankment, a set of differential settlement gauges was installed to measure the compression of each Pleistocene clay layers, such as Ma12 and Ma11U, Ma11L, Ma10 and the below Ma9. As shown in Fig. 13, as it is a pity that the continuous measurement could not be done in this site, we can get only the total settlement of the Pleistocene deposits during the 1st and 2nd filling and the differential settlements together with those summation during embankment construction. It should be noted that a large amount of settlement continues for the Pleistocene deposits, particularly, even below Ma9, non-negligible long-term settlement takes place with the elapsed time.

4.2 Finite element analysis assessing the in-situ performance of the reclaimed foundation

One-dimensional finite element analysis is adopted in the present study to assess the long-term settlement of Maishima Reclaimed Island. The adopted subsurface condition is shown in Fig. 14. As is clearly seen in Fig. 14 that the sand layers in Osaka Port is thick and their continuity is guaranteed (Kaitei Jiban, 1995). Then, one-dimensional approach can be accepted because the effect of the permeability boundary and mass permeability is unnecessary to be taken into account.

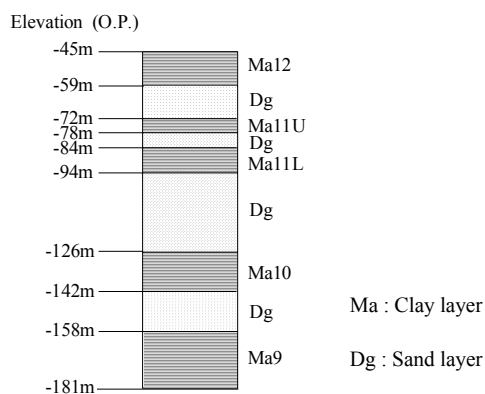


Fig. 14 Subsurface model for Maishima Reclaimed Island

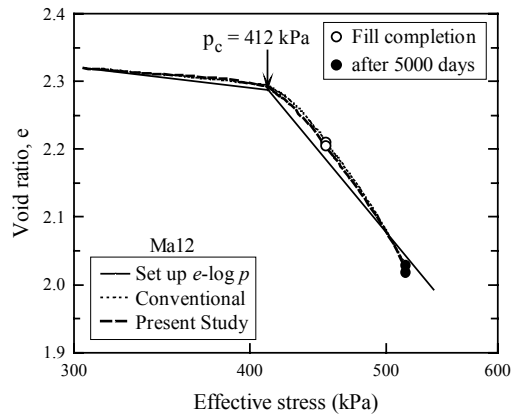
The soil parameters required for the input to the finite element code were determined rationally based on the prescribed procedure (Mimura et al., 1990). The set of parameters are shown in Table 1. In the present analysis, the above-mentioned new procedure is adopted, namely, the compression curve in the quasi-overconsolidated region with the inclination of $\kappa = \lambda/10 = \lambda_{OC}$ is assumed to have viscoplastic component as same as in the NC region. It should be noted that $e - \log p$ relation for the corresponding Pleistocene clays is unchanged at all except the virgin compression contains irreversible time-dependent behavior. The values of α , t_c and \dot{v}_0 related to the time-dependent behavior are determined as described in chapter 2.3. In the present analysis, it is assumed that the values of α in the quasi-overconsolidated region increase linearly with the increase in the relative yield stress index from $0.1\alpha_{NC}$ where the stress condition is equal to the overburden stress, p_0 . The values of \dot{v}_0 then in the quasi-overconsolidated region increase linearly as same as the proportion of the increase of α .

4.3 Results and discussions

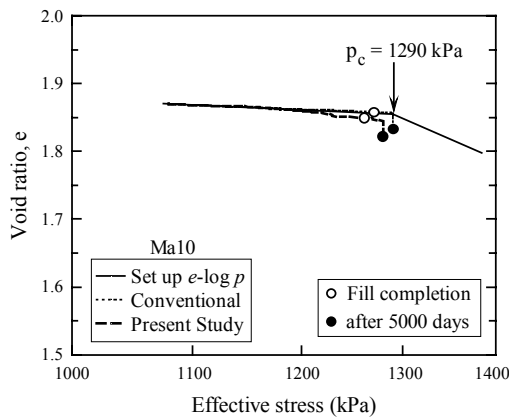
Fig. 15 shows the calculated $e - \log p$ relations during reclamation at Maishima. In all figures, the setup compression curves are illustrated by the solid lines, the results by the conventional and the present elasto-viscoplastic FEM are shown by the dotted and hatched lines. Ma12 in Fig. 15(a) is a representative of the Pleistocene clay layers that undergoes plastic yielding. It can be seen that the calculated $e - \log p$ relation with the present procedure is almost same as that of the conventional elasto-viscoplastic analysis. Ma10 in Fig. 15(b) is a representative of those layers that the final stress becomes close to p_c and Ma9 in Fig. 15(c) is a representative of those layers that the final stress remains less than p_c respectively. In all cases, the calculated compression curves in terms of $e - \log p$ relations move a slightly lower than the setup $e - \log p$ curves whereas those by the conventional FEM are almost move on the setup curves. It is natural that the time-dependent behavior such as shown in Fig. 15 takes place because the present procedure assumes that the time-dependent behavior occurs even in the quasi-overconsolidated region. Due to the assumption introduced in the present study, the advance in compression of the Pleistocene clays in the region less than p_c is found to be described.

The calculated performance is compared with the

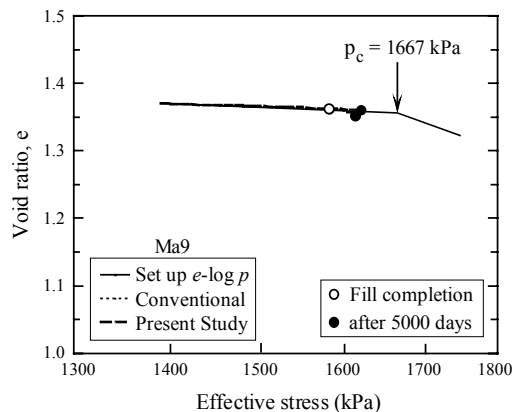
measured settlement for each layer in Fig. 16. Here, the solid lines denote the results of the present study while the hated lines are those by the conventional FE analysis. For Ma12 and Ma11U, the calculated and measured results show a good match. As is seen from Fig. 15(a), the upper Pleistocene clay layers such as Ma12 and 11 undergo the plastic yielding due



(a) Ma12



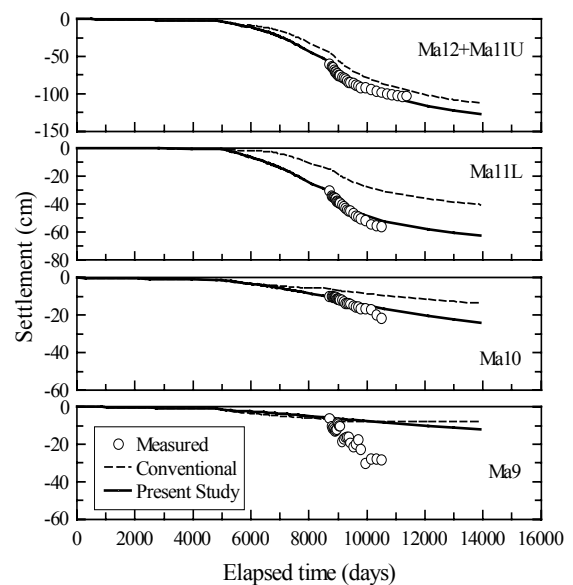
(a) Ma10



(a) Ma9

Fig. 15 Calculated compression curves, e - $\log p$ relations for Ma12, Ma10 and Ma9 at Maishima Reclaimed Island

to reclamation work. So, it is very natural that the calculated performance by both the conventional and the proposed procedures can well describe the stress - deformation characteristics of those clay layers Ma12 and 11U that become normally consolidated. On the other hand, the different behavior is expected in Ma11L, Ma10 and Ma9 the stress levels of which are close to p_c and less than p_c . For Ma11 and 10, the calculated performance with the proposed procedure shows much better coincidence with the measured settlement, whereas the conventional approach shows a remarkable underestimation. As for the settlement of Ma9, the calculated performance with the proposed procedure shows larger settlement than that by that with the conventional elasto-viscoplastic FEM because of the introduction of the time-dependent behavior in the quasi-overconsolidated region. But here, as it is impossible to separate the contribution of Ma9 itself from the measured data, the comparison of the calculated performance for Ma9 to the measured data is not appropriate. However, the measured amount of settlement taken place below Ma9 is more than 20cm in this limited monitoring period. Although it is not so clear that which layers in the lower Pleistocene clay deposits are affected by the reclamation load, it is very serious that such deeply sedimented Pleistocene clays can contribute the advance in settlement.



*measured data for Ma9 include the settlement of underlying layers

Fig. 16 Comparison of advance in settlement for each Pleistocene clay layer

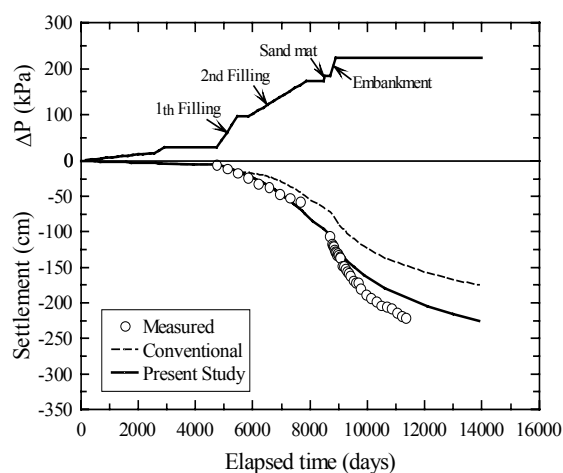


Fig. 17 Comparison of advance in total settlement for Pleistocene clay deposits

Fig. 17 shows the advance in the settlement of the Pleistocene deposits. Attention should again be paid to the fact that the measured data contains the contribution by the layers below Ma9. But, the calculated performance with the proposed procedure can describe the settlement of the Pleistocene deposits much better than that with the conventional FEM.

5. Conclusions

Long-term settlement has taken place in many coastal reclaimed foundations for over 20 years along Osaka Bay. Some examples of such serious long-term settlement were shown by the monitored data from Sakishima, Maishima and Yumeshima Reclaimed Islands in Osaka Port. Settlement occurred even now due to the compression of the highly structural Pleistocene clays. The monitored data from those reclaimed islands provided the fact that the Pleistocene clay layers have seriously been compressed even when the total overburden, $p_f (=p_0 + \Delta p)$ was less than p_c . Furthermore, the deep Pleistocene clay layers such as Ma9 and its underlying layers exhibited relatively large settlement. It should be noted that the measurement of the only total settlement does no longer make sense to know what actually happens in the marine foundations. The detailed measurement is indispensable for each affected layers together with the stress information such as pore water pressure to evaluate the behavior of those quasi-overconsolidated Pleistocene clays.

A new procedure is introduced to describe the

time-dependent compression of the Pleistocene clays in Osaka Bay. The assumption that an elasto-viscoplastic behavior takes place even in the region less than p_c as well as in the normally consolidated region is adopted and implemented into the elasto-viscoplastic finite element code. The experimental results for long-term one-dimensional consolidation tests are calculated with the proposed method and it is found that the remarkable time dependent compression in the region less than p_c is well predicted by the calculated performance. The Pleistocene clays in Osaka Bay exhibit a remarkable time-dependent compression curves in terms of $\varepsilon - \log p$ relations with respect to the strain rate. The calculated performance can also well describe those compression curves both for Ma12 and Ma 10. Here the variation of the secondary compression index, α is assumed to be proportional to the relative yield stress index. The framework adopted in the calculation for the laboratory experiments are also extended to the analysis of the in-situ long-term settlement at Maishima Reclaimed Island. The calculated $e - \log p$ relations for each clay layers with the proposed method naturally show almost the same for normally consolidated clays such as Ma12 as those with the conventional elasto-viscoplastic analysis. On the other hand, in the case that the stress condition of clays remains less than p_c , the present analysis shows the remarkable delayed compression with elapsed time even in the region less than p_c while the conventional analysis describes the typical elastic deformation with no gain in time dependent strain at all in this region. The calculated results for settlement can predict the in-situ measured settlement for each clay layer such as Ma12, 11 and 10 irrespective of the final stress conditions with the proposed method although the conventional analysis definitely underestimates them. From these results, the conventional procedure, such as elastic - elasto-viscoplastic approach is found to hold serious limitation to assess the long-term settlement taken place in Osaka Bay. Then, it is confirmed that the proposed procedure assuming that the elasto-viscoplastic behavior takes place in the region less than p_c as well as normally consolidated region is valid and functions well to assess the in-situ time-dependent long-term settlement occurred in the reclaimed area in Osaka Bay.

Reference

- Akai, K. and Tamura, T. (1976): An application of nonlinear stress-strain relations to multi-dimensional consolidation problems, *Annals DPRI, Kyoto University*, 21(B-2), pp. 19-35 (in Japanese).
- Bjerrum, L. (1967): Engineering geology of Norwegian normally-consolidated marine clays as related to settlements of buildings (7th Rankine Lecture), *Geotechnique*, Vol. 17, No. 2, pp.83-117.
- Christian, J.T. (1968): Undrained stress distribution by numerical method, *Journal of the Geotechnical Engineering Division, ASCE*, 94 (SM6), pp. 1333-1345.
- Ishii, I., Ogawa, F. and Zen, K. (1984): Engineering properties of marine clays in Osaka Bay (Part 2), Physical properties, consolidation characteristics and permeability, *Technical Note of the Port and Harbour Research Institute, Ministry of Transport*, 498, pp. 47-86 (in Japanese).
- Kaitei Jiban –Osaka Bay- (1995): Kansai Branch, JGS, (in Japanese).
- Kobayashi, G., Mitamura, M. and Yoshikawa, S. (2001): Lithofacies and sedimentation rate of quaternary sediments from deep drilling cores in the Kobe area, Southwest Japan, *Earth Science*, Vol. 55, pp.131-143 (in Japanese).
- Mesri, G. and Godlewski, P. M. (1977): Time and stress compressibility interrelationship, *Journal of the Geotechnical Engineering Division, ASCE*, 103 (GT5), pp. 417-430.
- Mimura, M. and Sekiguchi, H. (1986): Bearing capacity and plastic flow of a rate-sensitive clay under strip loading, *Bulletin of DPRI, Kyoto University*, 36(2), pp. 99-111.
- Mimura, M., Shibata, T., Nozu, M. and Kitazawa, M. (1990): Deformation analysis of a reclaimed marine foundation subjected to land construction, *Soils and Foundations*, 30(4), pp. 119-133.
- Mimura, M., Oda, K., Takeda, K., Yamamoto, K. and Fujiwara, T. (2001a): Compression properties and settlement behavior of Pleistocene marine clay deposits due to reclamation in Osaka Bay, *Proc. 46th JGS Geotechnical Symposium*, pp. 99-102 (in Japanese).
- Mimura, M., Ohshima, A., Takeda, K., Yoshikawa, M., Suwa, S. and Nagaya, J. (2001b): Settlement behavior of Pleistocene deposits due to reclamation in Osaka Port, *Proc. National Conf., JGS*, pp. 1007-1008 (in Japanese).
- Sekiguchi, H. (1977): Rheological characteristics of clays, *Proc. 9th ICSMFE*, 1, pp. 289-292.
- Sekiguchi, H., Nishida, Y. and Kanai, F. (1982): A plane-strain viscoplastic constitutive model for clay, *Proc. 37th Natl. Conf., JSCE*, pp. 181-182 (in Japanese).
- Research Committee of Seabed Deposits in Osaka Bay. (2002): *Seabed Marine Foundations -Development of Bay Area-* pp. 660 (in Japanese).

要旨

過圧密領域においても洪積粘土の時間依存性挙動が発生すると仮定した新たな圧縮モデルを提案し、長期圧密試験結果と大阪港舞洲洪積粘土地盤の沈下現象を弾粘塑性有限要素法によって解析した。その結果、過圧密領域でも正規圧密粘土と同様、時間の経過とともに圧縮が生じることになり、室内長期圧密試験結果、および従来モデルでは過小評価した大阪港舞洲埋立地下部洪積粘土層の沈下量を、精度良く表現できることがわかった。

キーワード：時間依存性挙動，擬似過圧密粘土，弾粘塑性 FEM，沈下